Proc. Natl. Acad. Sci. USA
Vol. 89, pp. 10099–10103, November 1992
Biochemistry

Structural analysis of ternary complexes of vaccinia RNA polymerase

(mRNA elongation/footprint/transcription bubble)

JEREMIAH HAGLER AND STEWART SHUMAN

Program in Molecular Biology, Sloan-Kettering Institute, New York, NY 10021

Communicated by Jerard Hurwitz, July 17, 1992

ABSTRACT **The structure of the elongation complex of vaccinia RNA polymerase halted at discrete template positions was examined by DNase I footprinting. The leading edge of the footprint bore a constant relationship to the catalytic template position, being 22–24 nucleotides (nt) in advance on the nontemplate strand and 17 nt on the template strand. DNase hypersensitivity of the nontemplate strand at the leading edge suggested that the DNA might be distorted as it entered the polymerase molecule. The region of DNA unwinding at the transcription bubble extended at least 12 nt 5′ from the catalytic center, as indicated by the reactivity of adenosine residues to diethylpyrocarbonate. Cu–phenanthroline-hypersensitive sites located 13 nt 5′ and 4 nt 3′ of the growing point appeared to demarcate the margins of the bubble. Strand asymmetry of chemical modification within the bubble was consistent with an RNA–DNA hybrid of no more than 10 base pairs.**

Transcription elongation complexes of *Escherichia coli* RNA polymerase have been characterized extensively *in vitro* (1–7). In eukaryotes, however, the daunting number of transcription initiation factors has complicated efforts to prepare promoter-specific RNA polymerase II elongation complexes from purified components. Alternatively, ternary complexes of RNA polymerase II have been studied in nuclear extracts (8) or in highly purified systems that circumvent the requirement for a promoter element (9). A more tractable model for study of mRNA elongation and termination is afforded by vaccinia RNA polymerase, a virus-encoded multisubunit homolog of cellular RNA polymerase II. Synthesis of vaccinia early mRNAs can be reconstituted *in vitro* with purified vaccinia RNA polymerase and a virus-encoded transcription initiation factor (VETF) composed of 82-kDa and 70-kDa subunits (10, 11). DNA templates containing a vaccinia early promoter linked to guanosine-lacking cassettes of various lengths (G*n*) have been used to prepare elongation complexes halted stably after incorporation of the first templated guanosine residue into the nascent RNA (12–14). The ternary complexes remain fully active insofar as they resume elongation upon adjustment of the nucleotide pool to override the elongation arrest. Probing the structure of such complexes as they move away from the promoter affords a dynamic view of RNA polymerase during transcription elongation (12). For example, ribonuclease footprinting of nascent mRNA revealed an RNA-binding site in the polymerase that encompasses an 18-nucleotide (nt) RNA segment extending 5′ from the growing point of the nascent transcript. We have now addressed by enzymatic and chemical footprinting the extent of DNA–protein interaction with each strand of the DNA template as well as the nature of the transcription bubble.

The publication costs of this article were defrayed in part by page charge payment. This article must therefore be hereby marked "*advertisement*" in accordance with 18 U.S.C. §1734 solely to indicate this fact.

MATERIALS AND METHODS

DNA Templates. Construction of the G*n* series of DNA templates for vaccinia early transcription and the nucleotide sequences of the promoter (identical for each template) have been described (12, 14). The nucleotide sequences of the initial transcribed regions (nontemplate strand) beginning at the +1 initiation site were as follows:

(G21) ATAACCCACTTCTATCACTAGGGG
(G34) ATAACCCACTTCTATCACTAACTTCTATCACTAGGG
(G51) ATAAACTTCTATCACTACTATCACTCAACTTCTATCACTACTATCACTCAGG.

The nucleotide sequence 3′ of the transcription arrest sites derived from the pBSKS+ plasmid and was identical for all templates used. 3′-Labeling of isolated restriction fragments containing the G*n* cassette was accomplished by using Klenow DNA polymerase and [α-^{32}P]dGTP. Strand-specific 5′-end-labeling of DNA was achieved by 30 cycles of PCR amplification of G*n* plasmid DNA in the presence of M13 forward- and reverse-sequencing primers, one of which had been 5′ ^{32}P-labeled with polynucleotide kinase.

Enzymes and Assays. RNA polymerase (phosphocellulose fraction, containing VETF in limiting amounts) was isolated as described (13). One unit of VETF was the amount sufficient to shift one fmol of radiolabeled DNA from free to protein-bound form, as measured by native gel electrophoresis. Complete DNA-binding/transcription reaction mixtures (20 μl) contained 20 mM Tris·HCl (pH 8.0), 9 mM $MgCl_2$, 2 mM dithiothreitol, 4–5 fmol of G*n* DNA, 0.13 unit of RNA polymerase, 4 units of VETF, 1 mM ATP, 1 mM CTP, 1 mM UTP, and 0.1 mM 3′-*O*-methylguanosine triphosphate (unless indicated otherwise). For gel-mobility-shift assays, the mixtures also contained 5% (vol/vol) glycerol. Incubation was for 10 min at 30°C. Protein–DNA complex formation was detected by electrophoresis of the samples through a nondenaturing 4% polyacrylamide gel containing 0.25× TBE (1× TBE is 90 mM Tris/64.6 mM boric acid/2.5 mM EDTA, pH 8.3). Enzymatic footprinting was done by adding 1 ng of DNase I with further incubation for 2 min at 30°C. Reactions were terminated by adjustment to 10 mM EDTA and 0.1% Sarkosyl. Chemical nuclease footprinting was performed by treating the reaction mixtures with 200 μM 1,10-phenanthroline, 45 μM $CuSO_4$, and 5 mM mercaptopropionic acid. Reactions were terminated after 4 min at 30°C by adding neocuproine·HCl to 2 mM. Diethylpyrocarbonate (DEP) modification was done by adjusting the binding reaction mixtures to 5% DEP with further incubation for 10 min at 30°C. DNA was recovered in each case by phenol/chloroform extraction and ethanol precipitation. Nuclease cleavage products were analyzed by electrophoresis through a denaturing 8% polyacrylamide gel. DEP-modified samples were cleaved with piperidine before electrophoresis.

Abbreviations: nt, nucleotide(s); DEP, diethylpyrocarbonate; VETF, virus-encoded transcription factor.

RESULTS AND DISCUSSION

Transcription Complex Formation. The first step in vaccinia early transcription is the binding of VETF to the promoter to form a preinitiation complex (10, 11, 13). Complex formation on radiolabeled G21 template was manifest as the appearance of a different species of retarded mobility during native gel electrophoresis (Fig. 1*A*, lane 2). RNA polymerase associated with the preinitiation complex in the presence of ATP, CTP, UTP, and 3′-*O*-methylguanosine triphosphate to form a ternary complex (lane 3). That this higher-order complex did, indeed, contain RNA was confirmed by incubating RNA polymerase with unlabeled G21 template and NTPs, including [α-^{32}P]CTP. The labeled nucleotide was associated with a complex identical in mobility to that of the presumptive ternary complex (lane 7). Formation of the CMP-labeled complex required RNA polymerase, template DNA, and ATP. Recovery of the labeled material from the gel-purified complex revealed incorporation of the precursor into a major RNA product corresponding to the 3′-*O*-methyl-G21 transcript (Fig. 1*B*).

Efficiency of template use by the RNA polymerase preparation could be enhanced by increasing the VETF level in the transcription reactions. Thereby, formation of a gel-stable ternary complex could be made virtually quantitative with respect to input DNA (Fig. 1*C*, lanes 4 and 8). This feature of the vaccinia system greatly simplified structural analysis of the transcription complexes, insofar as the footprinting experiments described below could be done without need to resolve protein–DNA complexes from free DNA. The G51 template, unlike the G34 and G21 DNAs, yielded two major DNA–protein complexes (Fig. 1*C*, lane 8). The more slowly migrating species unique to the G51 reaction represented a ternary complex containing two RNA polymerase molecules. Analysis of CMP-labeled transcripts extracted from the slower G51–DNA ternary complex indicated that the "leading" polymerase was halted, as expected, at the G51 position, whereas a "lagging" polymerase molecule was situated at template sites clustered around position +20 to +25 (data not shown).

DNase Footprinting. Preinitiation complex formation by purified VETF on uniquely 3′-end-labeled G34 template resulted in protection of regions upstream and downstream of the +1 transcription initiation site from nuclease digestion (Fig. 2). On the template strand, the footprint extended from −34 to +17. Of particular interest was the dramatic induction of DNase I hypersensitivity in the vicinity of the +1 position on the template strand (denoted by asterisk in Fig. 2). VETF protected the nontemplate strand from −32 to +19. Certain positions within the protected region (e.g., −7 and +3) remained susceptible to DNase attack. No hypersensitivity was noted on the nontemplate strand.

DNase footprints of similar dimensions (≈50 bp) were observed when VETF bound to the G21 and G51 templates (Fig. 3 *A* and *B*, lanes 2), and for other synthetic templates for which the initial transcribed regions differed more substantially in sequence from that of G34 (data not shown). (Note that in the experiments shown in Fig. 3 and in all subsequent

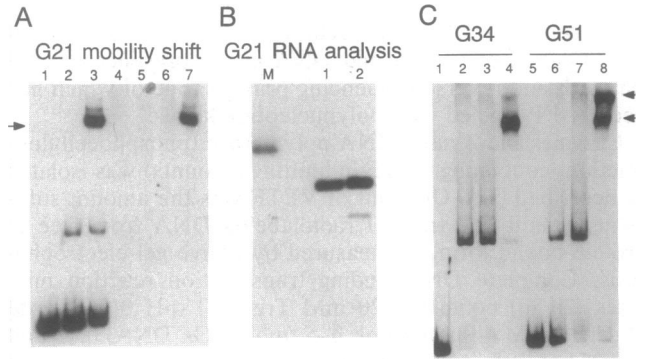

FIG. 1. Analysis of transcription complexes by native gel electrophoresis. (*A*) DNA-binding reaction mixtures contained 6 mM $MgCl_2$, 5 fmol of 3′ ^{32}P end-labeled 485-base pair (bp) *Pvu* II restriction fragment of G21 DNA template (lanes 1–3), proteins and NTPs as follows. Lanes: 1, protein omitted; 2, RNA polymerase; 3, RNA polymerase plus 1 mM ATP, 1 μM CTP, 0.1 mM UTP, and 0.1 mM 3′-*O*-methylguanosine triphosphate. The complete transcription reaction in lane 7 contained 5 fmol of unlabeled G21 *Pvu* II fragment, RNA polymerase, 1 mM ATP, 0.1 mM UTP, 0.1 mM 3′-*O*-methylguanosine triphosphate, and 1 μM [α-^{32}P]CTP (1000 Ci/mmol; 1 Ci = 37 GBq). Reactions lacking either DNA (lane 4), RNA polymerase (lane 5), or ATP (lane 6) were included as controls. Protein–DNA complexes were resolved by native gel electrophoresis. The ternary complex is indicated by the arrow. (*B*) CMP-labeled protein–DNA complex was excised from a native gel, and RNA was recovered by soaking the gel slice in 0.5 ml of 0.75 M ammonium acetate/1 mM EDTA, followed by ethanol precipitation. These transcripts were analyzed by electrophoresis through a denaturing 17% polyacrylamide gel (lane 2) alongside the CMP-labeled products of a transcription reaction not subjected to gel purification (lane 1). A 5′-labeled 24-mer DNA oligonucleotide was included as size standard (lane M). (*C*) 5′-End-labeled G34 (lanes 1–4) or G51 (lanes 5–8) DNA template was incubated without protein (lanes 1 and 5), in the presence of VETF (lanes 2 and 6), VETF plus RNA polymerase (lanes 3 and 7), or VETF, RNA polymerase, and 1 mM each of ATP, CTP, UTP, and 0.1 mM 3′-*O*-methylguanosine triphosphate (lanes 4 and 8). Samples were analyzed by native gel electrophoresis. Positions of ternary complexes are indicated at right by arrows.

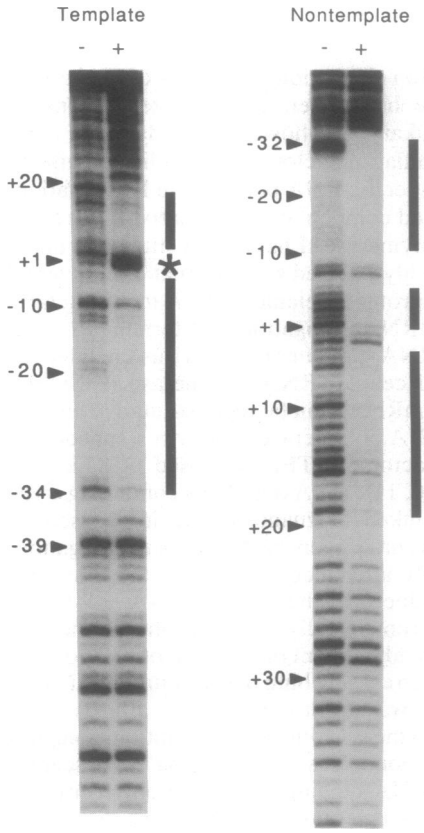

FIG. 2. DNase I footprinting of the preinitiation complex. DNA-binding reactions contained G34 DNA template (3′-end-labeled specifically in the template or nontemplate strand), 6 mM $MgCl_2$, and either no protein (−) or 4 units of VETF (+). Nucleotide positions relative to the +1 start site are indicated at left of each set of lanes. Regions protected by VETF from nuclease digestions are indicated by black bars. Sites of DNase hypersensitivity are denoted by an asterisk.

experiments we have used DNA templates uniquely labeled at the 5′ end.) The induction of nuclease hypersensitivity only on the template strand was observed consistently (Fig. 3), suggesting local distortion of the template upon VETF binding. By perturbing DNA structure specifically in the initiation region located between flanking sites of VETF–DNA interaction, the initiation factor may provide a docking site for RNA polymerase to access the preinitiation complex. Although the intrinsic ATPase activity of VETF (15) was required for initiation of RNA synthesis (13), the presence of ATP had no effect on the DNase I footprint or the induction of hypersensitivity by VETF on the template strand (data not shown).

Formation of the ternary complex upon provision of the NTPs effected a dramatic expansion of the region protected from nuclease digestion compared to that observed with VETF alone. On the nontemplate strand, recruitment of RNA polymerase to the G21 DNA was found to completely protect the region from +43 to −5 (Fig. 3*A*, lane 3), above and beyond the partial protection of the initial transcribed region seen in the preinitiation complex (lane 2). The leading edge of the polymerase protection was demarcated by an intense DNase I hypersensitive site (denoted by the open circle in Fig. 3*A*). (The apparent diminution of cleavage 3′ of the hypersensitive site was judged not to constitute true protection by the polymerase because this effect was not seen in other footprinting experiments with the G21 template.) Protected cleavage sites characteristic of the VETF footprint (e.g., near −30) persisted in the G21 ternary complex, suggesting that VETF remained bound in the elongation complex. Consequently, we assigned the −5 position as the minimum boundary of the lagging edge of the polymerase footprint.

The footprint of RNA polymerase paused on the G34 template extended from +56 to +8 on the nontemplate strand, again with a hypersensitive site in the vanguard (Fig. 3*A*). Comparison of the leading edges of the G21 and G34 footprints showed that the polymerase had moved down the DNA by an increment corresponding to the 13-nt difference in the size of the nascent transcripts. The VETF footprint in the vicinity of the start site, which was obscured by the polymerase footprint on the G21 DNA, reappeared in the G34 template, suggesting that polymerase might be bound in such a way as to superimpose itself on VETF and to slide past the initiation factor as elongation proceeded down the template. The footprint of the G51 complex extended from +75 back to +1 on the nontemplate strand; the incremental movement of the leading edge was again manifest in DNase I hypersensitivity. The larger dimensions of the G51 footprint likely reflected the presence of two polymerase molecules on many of the templates, as discussed above.

The RNA polymerase footprint on the template strand of the G21 DNA revealed a well-demarcated leading edge extending to position +38. The polymerase appeared to overlay the VETF footprint such that the signature VETF hypersensitive site in the +1 region was lost; thus, we estimated the lagging edge of the polymerase footprint to be at −2 (Fig. 3*B*). This represents a minimum estimate of the extent of upstream protection, as discussed below. The template-strand VETF-hypersensitive site was partially restored upon progression of the polymerase to the pause site at G34, again supportive of the retention of VETF at the promoter. The leading edge of the G34 footprint was at +51; the lagging edge was assigned at position +11, this being again a minimum estimate (Fig. 3*B*). The difference in the polymerase footprints of the G34 vs. G21 elongation complexes was thus commensurate with the size increase of the nascent RNA. The footprint of the G51 complex extended from +68 (leading edge) to −2 (estimated lagging edge) on the template strand.

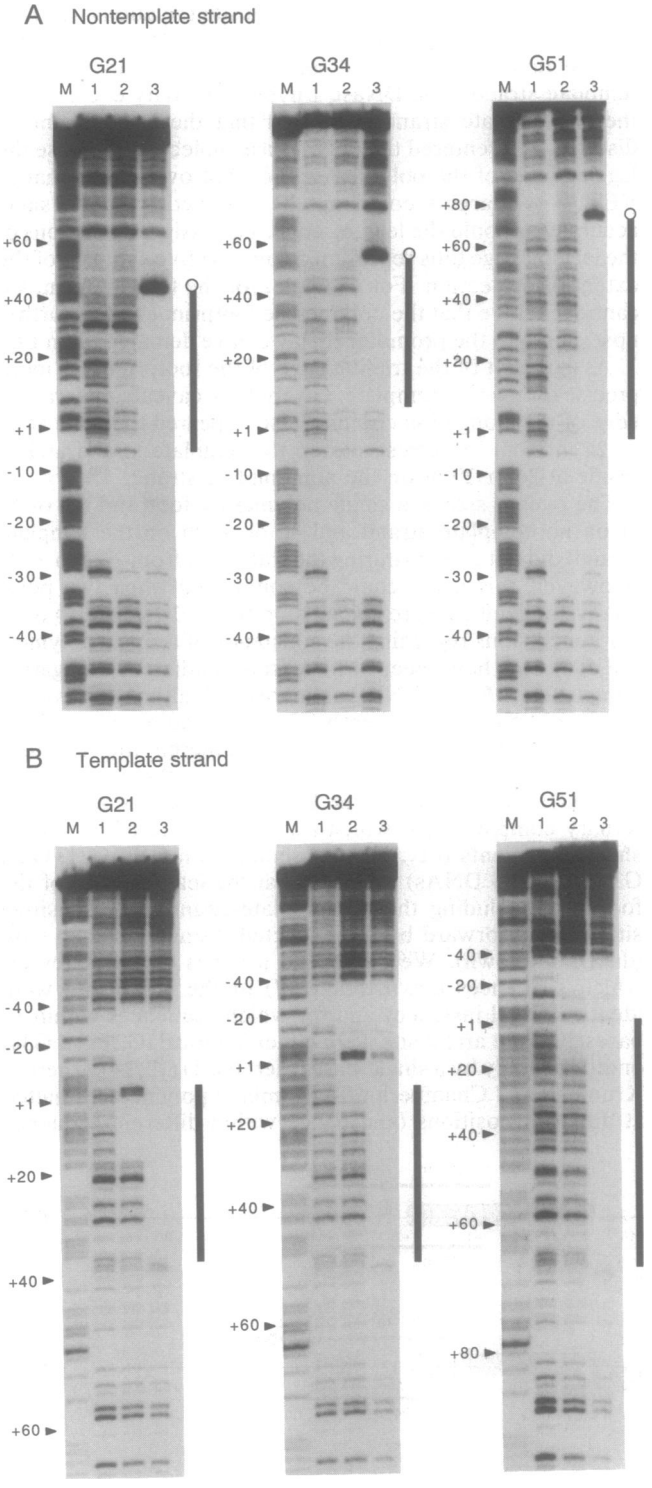

FIG. 3. DNase I footprinting of ternary complexes. DNA-binding reactions containing either no protein (lane 1), or VETF and RNA polymerase (lane 2), or VETF, RNA polymerase, and NTPs (lane 3) were incubated with G*n* template DNA 5′-end-labeled on the nontemplate strand (*A*) or the template strand (*B*) as indicated. Chemical sequencing ladders (A+G) were included as markers (lane M). Nucleotide positions relative to the +1 start site are indicated at left of each set of lanes. Black bars at right of each set of lanes indicate extent of protection by RNA polymerase within the ternary complex. Open circles indicate the position of ternary complex-dependent DNase I hypersensitivity.

When the dimensions of each footprint were expressed as the distance in nt from the known site of transcription arrest (Fig. 4), it became clear that the leading edge of the tran-

scription complex bore a virtually constant relationship to the catalytic template position—i.e., being 22–24 nt in advance on the nontemplate strand and 17 nt in advance on the template strand. The DNase I hypersensitivity exclusive to the nontemplate strand suggested that the DNA might be distorted as it entered the polymerase molecule. Because the lagging edge of the polymerase footprint overlapped that of VETF, its margins could not be assigned with the same accuracy as could the leading edge. The assigned positions of the lagging edge thus represent a conservative estimate of the extent of protection. For example, for the G21 footprint we cannot exclude that the polymerase footprint extends further upstream into the promoter than we have demarcated in Fig. 3. Assignment of the trailing edge of the footprint was more precise for the G34 template. Given these caveats, the trailing edge of the elongation complex also appeared to reside at 23 or 24 nt from the arrest site on the template strand and to reside at 26 or 27 nt on the nontemplate strand.

The overall size of a single polymerase footprint (48 or 49 nt on nontemplate strand and 40 or 41 nt on the template strand) did not change during the transition from +21 to +34. (However, this value could be compacted when two polymerase molecules were engaged on the G51 template.) Similar conclusions regarding the constancy of a single polymerase footprint have been drawn from studies of elongation complexes of *E. coli* RNA polymerase (4), although this view has been challenged recently (7). The leading edge of the vaccinia ternary complex did not undergo the saltatory contractions and expansions described for the bacterial enzyme (7). Comparisons of the DNase I footprints of vaccinia ternary complexes for which transcripts differed in size by short increments (i.e., those assembled on G17, G21, G27, G31, and G34 DNAs) revealed that the leading edge of the footprint (including the nontemplate-strand hypersensitive site) moved forward by the expected distance in each case (data not shown). We have used a series of templates for which sequences downstream (3′) of the arrest site were identical in all instances and for which sequences within 10 bases 5′ of the arrest site were either identical (G21 and G34) or differed only by a single-base insert (G51) (12, 14), whereas Krummel and Chamberlin (7) examined polymerases halted at different positions (and hence within different sequence contexts) on a single template. Whether the vaccinia elongation complex is subject to sequence-dependent conformation changes remains to be elucidated. However, our data make clear that there was no alteration of the ternary complex footprint as a function of distance moved away from the promoter.

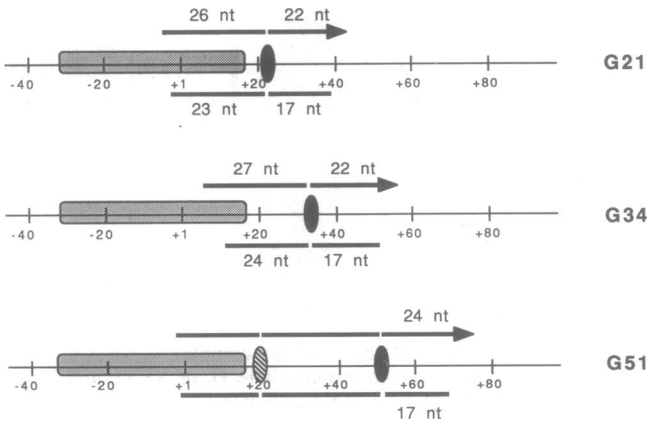

FIG. 4. Movement of the ternary complex along DNA during RNA chain elongation. DNase footprints of the G21, G34, and G51 ternary complexes are depicted. VETF footprint is indicated by the shaded rectangle. The catalytic center of RNA polymerase at the pause site is indicated by black and hatched ovals. Template coordinates are given relative to the transcriptional start site. Extents of the nontemplate-strand and template-strand footprints of RNA polymerase are shown above and below the linear DNA; these are expressed as the distance (in nt) of the footprint margins from the arrest site. DNase hypersensitivity on the nontemplate strand is indicated by an arrowhead.

Chemical Footprinting. We next used the chemical nuclease Cu–phenanthroline (16) to probe at higher resolution the interaction of the transcriptional apparatus with G21 DNA (Fig. 5). The chemical-cleavage pattern of the template strand generated in the presence of VETF and RNA polymerase without NTPs was essentially the same as that of DNA alone. This result was from disruption of the preinitiation complex upon addition of Cu–phenanthroline (data not shown). Ternary complexes were more stable to this treatment, such that a region of protection from cleavage was observed surrounding the transcriptional arrest site that extended from +10 to at least +17 on the G21 template strand (Fig. 5 *Left*, lane 3). On the nontemplate strand a region of protection specific to the ternary complex was detected from at least +15 to +23 (*Middle*, lane 3). Sites hypersensitive to Cu–phenanthroline cleavage were seen on both DNA strands (denoted by open circles in Fig. 5). The template-strand hypersensitive site at +9 marked the 5′ boundary of the protected region, whereas the nontemplate-strand hypersensitive sites at +24 to +26 marked the 3′ edge of the protection. A chemical footprint of similar dimensions and with analogous hypersensitive borders was generated by RNA polymerase on the G34 elongation complex (shown for nontemplate strand in Fig. 5, *Right*), except that location of the footprint was shifted 13 nt in the 3′ direction. Movement of the chemical footprint was also evinced by the reappearance in the G34 complex of strong cleavage sites at +15 and +16 that were protected in the G21 complex. A site of Cu–phenanthroline cleavage at about +10 of the nontemplate strand of the G21 and G34 templates appeared to be protected in the context of the ternary

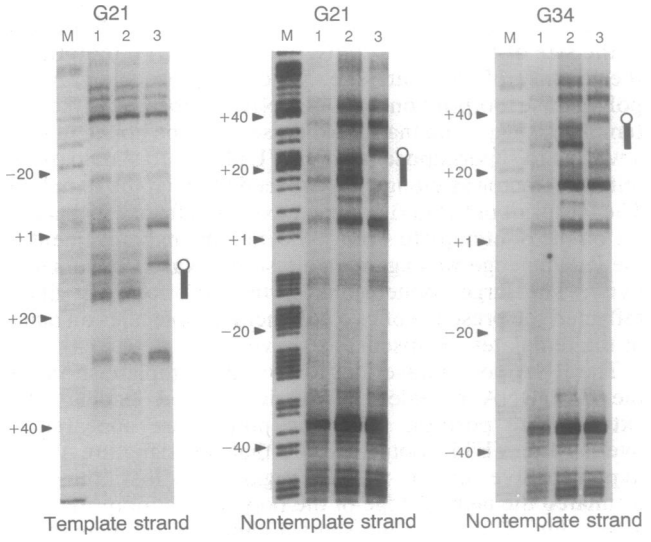

FIG. 5. Cu–phenanthroline footprint of ternary complexes. Binding reactions containing either no protein (lane 1), or VETF and RNA polymerase (lane 2), or VETF, RNA polymerase, and NTPs (lane 3) were incubated with either G21 or G34 template DNA 5′-end-labeled on either the template or nontemplate strand as indicated and then subjected to chemical nuclease treatment. Sequencing ladders (A+G) were included as size markers (lane M). Nucleotide positions are indicated at left of each set of lanes. Black bars indicate extent of protection by the ternary complex. Open circles indicate positions of Cu–phenanthroline hypersensitivity. (In the experiments in *Center* and *Right*, amount of strand cleavage was greater without protein; thus, longer cleavage products were underrepresented in the samples shown in lanes 1 relative to those in lanes 2 and 3.)

complex. As there was no change at this site accompanying polymerase movement, this effect could have been caused by VETF, which may be less prone to dissociation by the chemical treatment when in the ternary complex compared to the preinitiation complex.

DEP, which modifies adenosine residues preferentially at unpaired positions in duplex DNA, was used to probe the vaccinia elongation complex paused on the G21 DNA (Fig. 6); this approach had been applied previously to analysis of RNA polymerase I transcription complexes (17). We observed increased reactivity to DEP at three specific adenosine residues (+14, +17, and +20) on the nontemplate strand of the vaccinia ternary complex; two reactive adenosine residues (at +10 and +11) were detected on the template strand. An identical pattern of DEP reactivity was found for the G34 elongation complex, except that location of the footprint was shifted 13 nt downstream (data not shown).

Structure of Transcription Bubble. Sites of DEP sensitivity and Cu–phenanthroline hypersensitivity on the G21 elongation complex suggested a model for the transcription bubble illustrated in Fig. 7. The region of unpaired DNA, defined by DEP sensitivity of the adjacent adenosine residues at +10 and +11 on the template strand, necessarily extended at least 12 nt 5′ from the 3′-OH terminus of the nascent RNA chain. DEP modification was observed at all possible adenosine positions of the nontemplate DNA strand within this region; yet this modification was not detected at three template-strand adenosine residues located at +13, +15, and +19. Protection from DEP modification at template-strand bases within the bubble can be attributed either to an RNA–DNA hybrid or to solute exclusion by RNA polymerase bound to

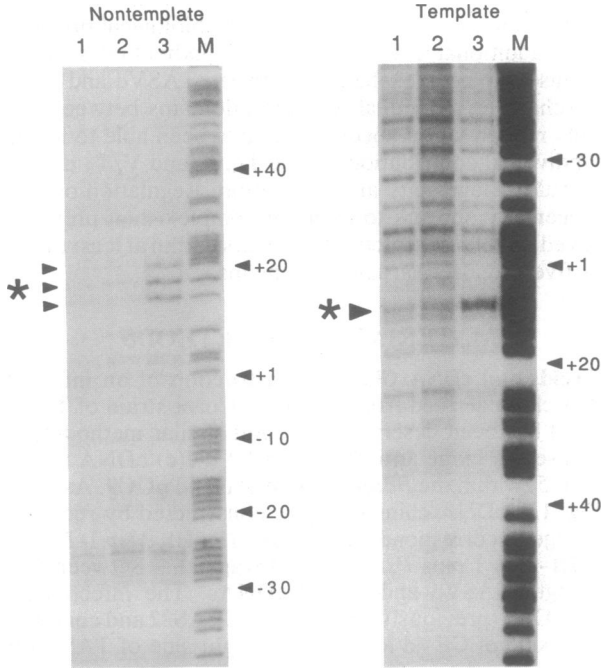

FIG. 6. DEP-reactive adenosines identify the transcription bubble. Binding reactions containing either no protein (lanes 1), or VETF and RNA polymerase (lanes 2), or VETF, RNA polymerase, and NTPs (lanes 3) were incubated with G21 template DNA 5′-end-labeled either on the template or nontemplate strands as indicated and then modified with DEP. Chemical sequencing ladders (A+G) were included as markers (lanes M). Nucleotide positions are indicated at right of each set of lanes. DEP-sensitive sites are indicated by an asterisk and arrowheads at left.

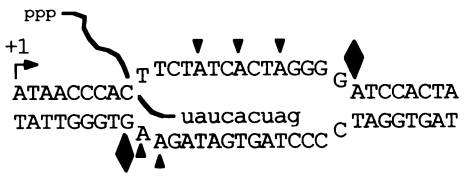

FIG. 7. Structure of the G21 transcription bubble. DNA sequence of the G21 template in the region of the arrest site is shown. DEP-sensitive adenosines are indicated by arrowheads. Sites hypersensitive to Cu–phenanthroline cleavage are marked by solid diamonds. The nascent RNA chain is shown in lowercase letters as a putative hybrid with the template strand. ppp, triphosphate.

the template strand. If the former scenario applied, we conclude that the RNA–DNA hybrid can be no more than 10 bp long (Fig. 7). The sites of hypersensitivity to Cu–phenanthroline may arise from distortions of the DNA helix at the duplex margins of the bubble (16). Such sites were located 13 nt 5′ and 4 nt 3′ of the RNA growing point.

Our model for the vaccinia transcription bubble is similar to structures proposed for a 17- or 18-nt bacterial transcription bubble based on topological analysis and on *in vivo* and *in vitro* footprinting studies (5, 6, 18). The transcription bubble of yeast RNA polymerase III paused at a single site *in vitro* is at least 13 nt but no more than 17 nt in size (19). The length of the putative RNA–DNA hybrid is a matter of some controversy (9). Protection of template-strand bases within the bubble from single-strand-specific modifications like that described above has been reported previously in other polymerase systems. When lack of reactivity has been interpreted as indicative of hybrid formation, upper limits of 12 bp for *E. coli* RNA polymerase (18) and 7 bp for RNA polymerase III (19) have been suggested. The multisubunit RNA polymerases, which have conserved features at the level of subunit primary sequence, appear then to adopt fairly similar structures in the context of their respective elongation complexes. Ongoing analysis of the vaccinia transcription complex should provide valuable mechanistic insight into a eukaryotic polymerase devoted exclusively to the synthesis of mRNA.

1. Carpousis, A. J. & Gralla, J. D. (1985) *J. Mol. Biol.* **183,** 165–177.
2. Straney, D. C. & Crothers, D. M. (1985) *Cell* **43,** 449–459.
3. Krummel, B. & Chamberlin, M. J. (1989) *Biochemistry* **28,** 7829–7842.
4. Metzger, W., Schickor, P. & Heumann, H. (1989) *EMBO J.* **8,** 2745–2754.
5. Gamper, H. B. & Hearst, J. E. (1982) *Cell* **29,** 81–90.
6. Shi, Y., Gamper, H., Van Houten, B. & Hearst, J. E. (1988) *J. Mol. Biol.* **199,** 277–293.
7. Krummel, B. & Chamberlin, M. J. (1992) *J. Mol. Biol.* **225,** 239–250.
8. Linn, S. C. & Luse, D. S. (1991) *Mol. Cell. Biol.* **11,** 1508–1522.
9. Rice, G. A., Kane, C. M. & Chamberlin, M. J. (1991) *Proc. Natl. Acad. Sci. USA* **88,** 4245–4249.
10. Broyles, S. S., Yuen, L., Shuman, S. & Moss, B. (1988) *J. Biol. Chem.* **263,** 10754–10760.
11. Broyles, S. S., Li, J. & Moss, B. (1991) *J. Biol. Chem.* **266,** 15539–15544.
12. Hagler, J. & Shuman, S. (1992) *Science* **255,** 983–986.
13. Hagler, J. & Shuman, S. (1992) *J. Virol.* **66,** 2982–2989.
14. Hagler, J. & Shuman, S. (1992) *J. Biol. Chem.* **267,** 7644–7654.
15. Broyles, S. S. & Moss, B. (1988) *J. Biol. Chem.* **263,** 10761–10765.
16. Sigman, D. S. (1990) *Biochemistry* **29,** 9097–9105.
17. Bateman, E. & Paule, M. R. (1988) *Mol. Cell. Biol.* **8,** 1940–1946.
18. Kainz, M. & Roberts, J. (1992) *Science* **255,** 838–841.
19. Kassavetis, G. A., Braun, B. R., Nguyen, L. H. & Geiduschek, P. E. (1990) *Cell* **60,** 235–245.